

Phenomenology of the dispersion relation in quantum space

Michaela Ďuríšková,^b Samuel Kováčik^{a,b} and Patrik Rusnák^{a,*}

^a*Department of Theoretical Physics, Faculty of Mathematics, Physics and Informatics,
Comenius University in Bratislava,
Mlynská dolina, 842 48, Bratislava, Slovakia*

^b*Department of Theoretical Physics and Astrophysics, Faculty of Science, Masaryk University,
Brno, Czech Republic
E-mail: rusnak57@uniba.sk, samuel.kovacik@fmph.uniba.sk,
505876@mail.muni.cz*

The idea of quantum space was proposed long ago, but directly measuring its effects remains far in the future — simply because we cannot yet generate the energies required to prove it. Fortunately, even though the effects of such a structure are minimal, under certain conditions we can make use of the best high-energy generator available: the Universe itself, which regularly produces powerful high-energy bursts. If those bursts originate from distant sources, the tiny effects of quantum space can accumulate over long distances into a measurable magnitude. Many studies in this field rely on perturbative methods, typically considering only first- or second-order corrections. However, this work employs a full dispersion law derived from a three-dimensional quantum space model. Our primary focus is investigating the phenomena of in-vacuo dispersion and the threshold anomaly. We also briefly consider how additional spatial dimensions might influence the behavior of such a quantum space.

*Proceedings of the Corfu Summer Institute 2024 "School and Workshops on Elementary Particle Physics and Gravity" (CORFU2024) 12 - 26 May, and 25 August - 27 September, 2024
Corfu, Greece*

*Speaker

1. Introduction

The concept of quantum space emerged soon after the development of quantum mechanics. It is generally anticipated that the effects of quantum spacetime structure would manifest at the Planck scale. However, the energies currently accessible in experiments – such as those at the LHC, where $E_{\text{LHC}} \approx 10^{13} \text{eV}$ – are vastly lower than the Planck energy, $E_P \approx 10^{28} \text{eV}$. Despite this gap, a minimal length scale has gained considerable attention. Hossenfelder [1] has comprehensively reviewed this feature, while Amelino-Camelia [2] and an expanding community have explored various phenomenological scenarios in this context.

Quantum space gives rise to numerous effects that are extremely difficult to observe. Fortunately, a few of these effects are within our observational reach. This work will focus on two phenomena associated with Gamma-Ray Bursts (GRBs). The first is the wavelength-dependent vacuum velocity, which can measurably influence particles moving at the speed of light. The second is the so-called Threshold Anomaly, a phenomenon we began exploring following the high-energy gamma-ray burst GRB221009A, which had an energy of $E_{\text{GRB}} = 18 \text{TeV}$. This energy is comparable to that of the LHC, with the key difference being that its source was located 2.4 Gly away, providing the necessary conditions for the quantum space effect to accumulate.

Many papers in this field typically focus on a few orders of magnitude, which is justified since E/E_F tends to be small. Here, E_F represents the fundamental energy scale, which may but does not necessarily, correspond to the Planck scale. In contrast, we have utilized the whole relation derived from 3-dimensional quantum space R_λ^3 . More information about physics discussed in this work can be found in [3].

2. Vacuum dispersion from quantum space R_λ^3

In quantum space theories, the exact position of a particle cannot be measured. This fact leads us towards noncommutative spaces. Motivated by the phase space of a free particle, where the Heisenberg uncertainty principle prevents simultaneous measurement of position and momentum, we define noncommutative space similarly as

$$[\hat{x}_i, \hat{x}_j] = i\hat{\theta}_{ij} = 2i\lambda\epsilon_{ijk}\hat{x}_k. \quad (1)$$

Here, we define $\hat{\theta}_{ij}$ in such a way that rotational symmetry is preserved. It is evident that as $\lambda \rightarrow 0$, we recover the standard R^3 space. The closer analysis can be found in [4].

After some effort, the velocity operator can be derived. The relation between Hamiltonian and velocity operator is

$$\hat{H}_0 = \frac{1 - \sqrt{1 - m^2\lambda^2\hat{v}^2}}{m\lambda^2} = \frac{m\hat{v}^2}{2} + \frac{m^3\hat{v}^4}{8}\lambda^2 + \mathcal{O}(\lambda^4). \quad (2)$$

We can observe that limit $\lambda \rightarrow 0$ will recover standard relation for kinetic energy. We want to have a relation between Hamiltonian and momentum operator, so one can perform Legendre transformation $\hat{p} = \frac{\partial \hat{H}_0}{\partial \hat{v}} = \frac{m\hat{v}}{\sqrt{1 - m^2\lambda^2\hat{v}^2}}$, which will leave us with

$$\hat{H}_0 = \frac{1}{m\lambda^2} \left(1 - \sqrt{1 - \frac{\lambda^2\hat{p}^2}{1 + \lambda^2\hat{p}^2}} \right) = \frac{\hat{p}^2}{2m} - \frac{3\hat{p}^4}{8m}\lambda^2 + \mathcal{O}(\lambda^4). \quad (3)$$

The maximum achievable energy is given by $E_F = \frac{1}{m\lambda^2}$. This expression was derived within the framework of nonrelativistic quantum mechanics. However, we want our dispersion relation to remain sensitive to the scale E_F , which motivates us to adopt a relativistic expression by substituting $p^2/2m \rightarrow pc$. We will also restrict ourselves to energy (or momentum) eigenstates that satisfy $\hat{H}_0\Psi = E\Psi$. With these adjustments, we arrive at the relativistic dispersion relation

$$E^2(p) = E_F^2 \left(1 - \sqrt{1 - \frac{2pc}{E_F + 2pc}} \right)^2 = p^2 c^2 \left(1 - \frac{3pc}{E_F} + O(E_F^{-2}) \right). \quad (4)$$

The correction term is of the order of $O(E_F^{-1})$, which is expected. We assume this relation holds for any relativistic particle. However, this is done without access to a complete theory of quantum space – so modifications may still be necessary in the future.

3. Phenomenology

3.1 Flight time delay

A closer look at (4) reveals that photons with different wavenumbers propagate at different velocities. Higher-frequency waves travel faster or slower than lower-frequency ones, even in a vacuum, depending on the sign in front of the leading correction term. Gamma-ray bursts provide a valuable tool for studying in-vacuo dispersion. Imagine two photons emitted simultaneously from the same source but detected at different times. While the effect is minuscule, it can accumulate over vast distances. Following [2], we take the dispersion relation for massless particles to be

$$p^2 \simeq E^2/c^2 + \eta p^2 (E/E_F)^n. \quad (5)$$

The difference in arrival time between particles of different energies is

$$\Delta t \simeq \eta \frac{n+1}{2H_0} \frac{p^n}{E_F^n} \int_0^z dz' \frac{(1+z')^n}{\sqrt{\Omega_m(1+z')^3 + \Omega_\Lambda}}, \quad (6)$$

where $\Omega_m, \Omega_\Lambda, H_0$ are cosmological parameters.

We want to derive a similar formula for our dispersion relation. Firstly, we replace momentum with comoving momentum ap , perform Legendre transformation $v = \frac{\partial H}{\partial p}$, replace the scale parameter $a = \frac{1}{1+z}$ and finally integrate over to find the distance traveled by the particle

$$x(z, E) = \frac{c}{H_0} \int_0^z \left(\frac{E_F/(1+z')}{E_F/(1+z') + 2pc} \right)^{3/2} \frac{dz'}{\sqrt{\Omega_m(1+z')^3 + \Omega_\Lambda}}. \quad (7)$$

The difference in the arrival times of particles with different energies is given by

$$\Delta t(E_1, E_2, z) = -\frac{3c}{H_0} \frac{\Delta E}{E_F} \int_0^z \frac{(1+z') dz'}{\sqrt{\Omega_m(1+z')^3 + \Omega_\Lambda}} + O\left((E/E_F)^2\right), \quad (8)$$

where $E = pc$. Upon expanding in E , each term can be expressed in terms of hypergeometric functions. This result is consistent with the values reported in the literature.

3.2 Threshold anomaly

The other effect we are going to discuss is the threshold anomaly. In the previous discussion, we focused purely on photon propagation in vacuum. However, when considering interactions, the situation becomes more intricate — space is not truly empty but filled with a bath of background photons. Their origin may vary; for instance, we encounter photons from the cosmic microwave background (CMB) or the extragalactic background light (EBL). While these background fields were present before as well, their relevance becomes significant only when high-energy interactions are involved.

Let us consider the process $\gamma\gamma \rightarrow e^-e^+$. Assuming the standard dispersion relation, this process occurs when

$$E \geq E_{\text{th}} = \frac{m_e^2}{E_b}, \quad (9)$$

where m_e is a mass of the electron, E_{th} is the threshold energy of the high-energy photon, and E_b is the energy of the background photon. Considering CMB and EBL photons, there should be attenuation on scales ranging from Mpc to Gpc. An interesting observation was made when a photon with energy 18 TeV from GRB221009A was detected, originating from a distance of 724 Mpc. A possible explanation for this observation is the previously discussed modification of the dispersion relation.

Two photons can create a particle-antiparticle pair with mass $m = \sqrt{EE_b}/c^2$. If m is smaller than the mass of any particle allowed by conservation laws, then the process will not occur. If we fix E_b and gradually increase E , the process becomes unavoidable at some point, effectively making it impossible to observe photons beyond a certain energy threshold. However, when we consider a modified dispersion relation, space becomes transparent at high energies, allowing the detection of high-energy photons such as those observed from GRB221009A [5].

The minimal mass produced by a high-energy photon with energy $E = pc$ is

$$m = \frac{1}{2c^2} \sqrt{E^2(p) - (pc)^2 + 2E_b(E(p) + pc)} \approx m_0 \left(1 - \frac{3(pc)^2}{8E_F E_b} \right) + \dots, \quad (10)$$

where we have plugged in our dispersion relation (4) and substituted $m_0 = \sqrt{EE_b}/c^2$, which was threshold in unmodified relation. Results are sensitive to E_b and E_F , which analysis can be found in Table (1).

4. Observational technology

4.1 Flight time delay

Let us compare results from reference [6] with our results on the study of GRB221009A. In the reference, the authors have used the dispersion relation of the form

$$v(E) = c \left(1 - \frac{n+1}{2} \left(\frac{E}{E_F} \right)^n \right), \quad (11)$$

where we take $n = 1$, which closely resembles our relation, differing only by a factor of 3 in front of the leading correction term. This difference is negligible due to the ambiguity in the definition

$E_B \setminus E_F$ [MeV]	∞	E_{Pl}	$10^{-1}E_{Pl}$	$10^{-2}E_{Pl}$
1 eV	4.2	4.2	3.8	0.019
10^{-1} eV	1.3	1.2	0.0061	< 0
10^{-2} eV	0.42	0.0019	< 0	< 0
10^{-3} eV	0.13	< 0	< 0	< 0

Table 1: Mass of a particle produced via the interaction of an 18 TeV photon with a background photon of energy E_B , as given by relation (10), for various values of the fundamental energy scale E_F (measured in MeV/ c^2). In theories where the fundamental scale deviates significantly from the Planck energy, pair production is suppressed for all background photon energies. In contrast, when $E_F \sim E_{Pl}$, only low-energy background photons are excluded from the interaction. For larger values of E_B , the resulting mass exceeds the electron mass, $m_e = 0.511$ MeV/ c^2 , making pair production kinematically allowed.

of E_F . Values of the variables they used are $\Delta E = 99.3$ GeV, $E_F = 3.6 \times 10^{17}$ GeV, $H_0 = 67.3$ km s $^{-1}$ Mpc $^{-1}$, $\Omega_m = 0.315$, $\Omega_\Lambda = 0.685$. These values results in $\Delta t \approx 20$ s. If we use our relation (4) we will obtain $\Delta t \approx 60$ s. We can obtain similar values by taking the different values of the E_F . If we take $E_F \sim E_{\text{Planck}}$, the time delay will be $\Delta t \approx 1.83$ s. This effect can be measurable, but it requires identifying high- and low-energy photons emitted from the source simultaneously. Some efforts toward this have already been made in the previously mentioned reference.

To get a feeling about how to look at the technology, let us have a closer look at the small satellite detector *GRBAlpha* [7]. This satellite has a temporal resolution 1 s and energy limit 1 MeV. Timeshift for $E_F \sim E_{\text{Planck}}$ would be around $\Delta t \approx 10^{-5}$ s. Temporal resolution and energy limits can be found in Table (2).

	Temporal resolution	Energy range
GRBAlpha [7]	1 s	80 keV – 950 keV
Fermi GBM [8]	$2 \mu\text{s}$	8 keV – 40 MeV
Fermi LAT [8]	$< 1 \mu\text{s}$	20 MeV – 300 GeV
Hermes [9, 10]	≤ 250 ns	5 keV – 0.5MeV

Table 2: Technical limits of some GRB detectors.

4.2 Threshold anomaly

The reduced attenuation due to electron-positron pair production is another effect worth investigating. While this phenomenon is relevant for current astronomical observations, it may also become accessible in future laboratory experiments. Laboratory setups are particularly appealing, as the distribution of background photons in astrophysical contexts can be difficult to model accurately. There are two interesting approaches one could take. The first involves directing a source of gamma photons through an isolated chamber filled with low-frequency radiation (e.g., regular microwaves), thereby making the threshold condition in equation (9) experimentally relevant.

Another interesting possibility is to investigate pulsars — not extremely distant, but highly stable sources of gamma photons. One auspicious example is the Vela pulsar, which emits photons with energies around 20 TeV. The light from this source takes approximately 3×10^{10} s to reach

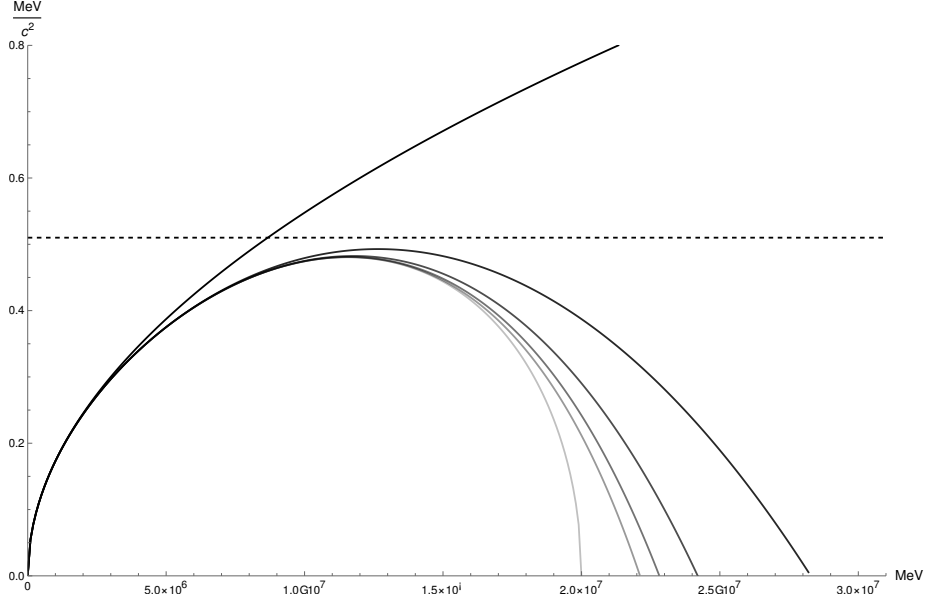


Figure 1: This plot shows the maximum mass producible via the classical relation from equation (10), assuming $E_F = 10^{22}$ MeV and a fixed background photon energy of $E_B = 3 \times 10^{-2}$ eV. The curves correspond to successive orders in the expansion of the expression in $1/E_F$, with darker grey indicating lower-order approximations and lighter grey representing higher-order corrections. The bottom-most curve represents the exact result, which sharply ends at 2×10^7 MeV — the maximal achievable value. The dashed horizontal line shows the electron mass. If the produced mass falls below it, pair production is not allowed. As the plot illustrates, for $E_F \approx E_{Pl}$, only very low-energy background photons are excluded from the process. For smaller values of E_F , however, the interaction becomes increasingly suppressed across a broader range of background photon energies.

us, and the pulsar spins at a frequency of about 10 Hz. Assuming the fundamental energy scale E_F is at the Planck scale and considering an energy difference $\Delta E \sim 10$ TeV, this would lead to a potential flight time delay of around 10^{-5} s. Such a delay should be within the resolution of current detection systems. Thanks to the source’s stability, there is a good chance to collect a robust dataset and perform cross-correlation analysis to look for energy-dependent time lags.

5. Conclusion

We have derived a dispersion relation from the quantum space R_λ^3 . While many other theories predict linear or quadratic corrections to the standard dispersion law, a series expansion of our relation is consistent with a linear correction.

We focused our analysis on two potentially measurable phenomena arising from this modified dispersion relation — flight time delay and threshold anomaly. Following similar steps as outlined in [6], we derived the expected delay between two photons of different energies emitted simultaneously from the same astrophysical source. We are entering an era when satellite observations may begin to shed light on the quantum nature of space – whether through the accumulation of minuscule effects over vast cosmic distances or through the (non)observation of high-energy photons predicted to be attenuated by the vacuum.

The calculated flight time delays in our model were in good agreement with values appearing in the literature. Additionally, our exploration of the threshold anomaly revealed several intriguing aspects. By considering various levels of approximation to the modified dispersion law, we observed distinct differences in predicted outcomes. This sensitivity suggests that threshold anomalies could serve as a tool to differentiate between competing models of quantum spacetime.

Looking forward, it is conceivable that future laboratory experiments – perhaps involving interactions between high- and low-energy photons under controlled conditions – might reach the precision necessary to test these predictions directly.

Acknowledgments

This research was supported by VEGA 1/0025/23 grant and MUNI Award for Science and Humanities funded by the Grant Agency of Masaryk University. The authors would also like to express gratitude to the organisers of the Workshop on Noncommutative and Generalized Geometry in String theory, Gauge theory and Related Physical Models.

References

- [1] S. Hossenfelder, Living Rev. Rel. **16** (2013), 2 doi:10.12942/lrr-2013-2 [arXiv:1203.6191 [gr-qc]].
- [2] G. Amelino-Camelia, Living Rev. Rel. **16** (2013), 5 doi:10.12942/lrr-2013-5 [arXiv:0806.0339 [gr-qc]].
- [3] S. Kováčik, M. Ďurišková and P. Rusnák, [arXiv:2402.05832 [gr-qc]].
- [4] S. Kováčik and P. Prešnajder, J. Math. Phys. **54** (2013) no.10, 102103 doi:10.1063/1.4826355.
- [5] H. Li and B. Q. Ma, J. High Energy Astrophys. **32** (2021), 1–5 doi:10.1016/j.jheap.2021.07.001.
- [6] J. Zhu and B. Q. Ma, J. Phys. G **50** (2023) no.6, 06LT01 doi:10.1088/1361-6471/accebb [arXiv:2210.11376 [astro-ph.HE]].
- [7] A. Pál *et al.*, Astron. Astrophys. **677** (2023), A40 doi:10.1051/0004-6361/202346182 [arXiv:2302.10048 [astro-ph.IM]].
- [8] D. J. Thompson and C. A. Wilson-Hodge, In *Handbook of X-ray and Gamma-ray Astrophysics* (2022), p.29 doi:10.1007/978-981-16-4544-0_58-1.
- [9] F. Fiore *et al.*, In *Space Telescopes and Instrumentation 2020: Ultraviolet to Gamma Ray*, Society of Photo-Optical Instrumentation Engineers (SPIE) Conference Series **11444** (2020), 114441R doi:10.1117/12.2560680 [arXiv:2101.03078 [astro-ph.HE]].
- [10] F. Fiore *et al.* [HERMES-SP and HERMES-TP Collaborations], In *SPIE Astronomical Telescopes + Instrumentation 2020* (2021) doi:10.1117/12.2560680 [arXiv:2101.03078 [astro-ph.HE]].